PROGRESS AND PERSPECTIVE FOR HIGH FREQUENCY, HIGH PERFORMANCE SUPERCONDUCTING ECR ION SOURCES

D. Leitner, J.Y. Benitez, M L Galloway, T.J. Loew, C.M. Lyneis, D.S. Todd, Lawrence Berkeley National Laboratory, One Cyclotron Road, Berkeley, California, 94720 U.S.A.

Abstract

Next-generation heavy ion beam accelerators require a great variety of high charge state ions with an order of magnitude higher beam intensity than is currently routinely available. Driven by this increasing demand for high performance ECR ion sources and enabled by advances in superconducting magnet technology, third generation superconducting (SC) ECR ion sources have been developed world-wide. The superconducting VENUS ECR ion source at the 88-Inch Cyclotron at the Lawrence Berkeley National Laboratory is the first ECR ion source designed for optimum operation at 28 GHz. Since it started operation in 2002 many world record ion beam intensities have been produced. VENUS has pioneered the field of high field SC ECR ion sources, and many of the design features and lessons learned during the VENUS commissioning phase have been incorporated in current 28 GHz ECR ion source projects such as GYRO-SERSE and SC-ECRIS. This paper will highlight recent progress on the VENUS ECR ion source for medium and high charge state production. In addition, it will discuss perspectives and main technical challenges of building 4th generation superconducting ECR ion sources using microwave heating frequencies of 56 GHz.

INTRODUCTION

ECR ion sources use magnetic confinement and electron cyclotron resonance heating to produce a plasma consisting of energetic electrons and relatively cold ions with an ion temperature of a few eV. The plasma electrons' energy distribution is non Maxwellian, but can be roughly characterized by three components: a cold population (~20 eV), which is important for the overall plasma density and confinement time; a warm population (up to 100keV), which is responsible for the ionization process; and a hot population with a high energy tail reaching up to several hundreds of keV, which is the main cause of x-ray bremstrahlung observed outside of ECR ion sources.

High charge state ions are primarily produced by sequential impact ionization. These ions must remain in the plasma long enough (tens of ms) to reach high charge states. The main parameter determining the performance of an ECR ion source is the product of the plasma density and ion confinement time ($n_e\tau_i$). Together with the neutral gas density in the plasma this product determines both the peak of the charge state distribution and the highest charge state that can be produced in the plasma. The extracted ion beam current (I_{ext}) for a particular ion is proportional to the ratio,

$$I_{ext} \propto \frac{n_{ion}^{CS}}{\tau_{ion}} \quad ,n_e = \sum_{CS}\sum_{ion} n_{ion}^{CS} \ , \qquad (1)$$

with n_{ion}^{CS} the density of a particular ion species of interest in charge state +CS, n_e the plasma density, and τ_{ion} the ion confinement time of this charge state. So if one could selectively decrease the ion confinement time, it would be easy to increase the extracted ion current. However, the ion confinement time and plasma density are strongly coupled and can't be adjusted independently. As a result, the trend for new ECR ion source construction has been to design for both the highest possible confinement fields and highest possible heating frequency. To optimize for a desired charge state during operation, the source is carefully balanced (tuned) between both parameters along with the neutral gas pressure in the plasma (see section 1). The rationale for this approach is based on the semi-empirical scaling laws formulated by Geller in 1986 [1] which state that the plasma density can be increased by increasing the microwave heating frequency ($n_e \sim \omega_{rf}^2$), while the ion confinement time increases with the radial and axial mirror ratio ($\tau_i \sim B_{max}/B_{min}$). Using these general principles, a number of high performance ECR ion sources have been developed over the last few decades which have established clear confining field guidelines for the design of high performance sources operating at any heating frequency. These field ratios are summarized in table , where the confining fields at the RF injection end (Binj), extraction end (Bext), and in the radial direction (Brad), are related to the resonant heating field (B_{ECR}) and one another. The resonant heating field is related to the angular frequency applied microwave heating, f_{rf}, by the $B_{ECR}=2\pi f_{rf}\ m\ /e$, where m the electron mass, and e the electron charge. For example, for 28 GHz the corresponding resonant magnetic field is 1 Tesla.

As the demand for high charge state ions continues to increase, third generation, high field superconducting (SC) ECR ion sources at frequencies of 18 to 28GHz are now emerging[2,3] and preliminary concepts for superconducting ECR ion sources beyond 28 GHz are being proposed[4,5].

Table 1: Typical magnetic field ratios for high performance ECR ion sources

B_{inj}/B_{ecr}	~ 4
B_{ext}/B_{ecr}	~ 2
B_{min}/B_{ecr}	~ 0.5 to 0.8
B_{rad}/B_{ecr}	≥ 2
B_{ext}/ B_{rad}	≤ 0.9 to 1

The VENUS ECR ion source at the Lawrence Berkeley National Laboratory (LBNL) is a 3rd generation source and has been designed for optimum operation using 28 GHz plasma heating frequency. It is currently the only superconducting, high field ECR ion source operating at this frequency. During design and construction, a number of the technical challenges with respect to the superconducting magnet design and construction, cryogenics and bremsstrahlung heating were encountered and had to be addressed. The solutions developed are now being incorporated in other superconducting ECR ion sources under design or construction such as MS-ECRIS, SC-ECRIS, and SuSI [6-9]. A similar set of challenges can be expected for the development of 4th generation ECR ion sources. Using the VENUS ECR ion source as an example and based on measurements performed with the source, these technical challenges and perspectives for designing 4th generation ECR ion sources are discussed in the third section. In first two sections a brief summary and update of the status and performance of the VENUS ECR ion source are described.

VENUS ECR ION SOURCE

.

Fig. 1 shows the mechanical layout of the VENUS ECR ion source. The mechanical design has been optimized for maximum ion source performance as well as easy serviceability for operational use. The maximum axial magnetic confinement fields are 4 T at injection and 3T at extraction and are generated by three solenoid coils. A wide range of minimum B fields (Bmin) between the magnetic mirrors can be tuned by changing the current of the middle coil. The radial field at the plasma chamber wall can be operated at fields up to 2.1 Tesla (slightly more than twice the resonant field for 28 GHz of 1T)) [10]

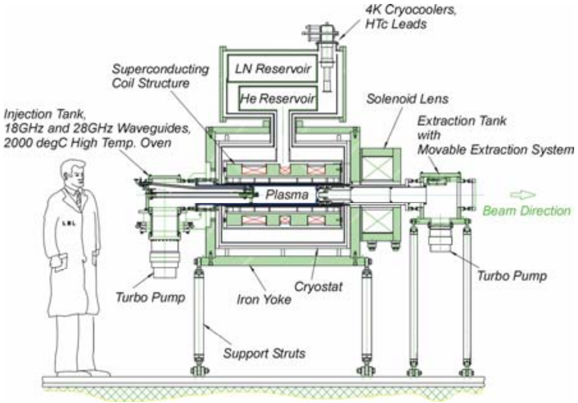

Figure 1: Mechanical layout of the VENUS ion source and cryogenic systems

VENUS has been operated routinely using 28 GHz as its main heating frequency since 2004 and has produced many record beams. Besides 28 GHz, 18 GHz can be injected as a second frequency for double frequency heating or used for single frequency heating ($B_{ECR,18\ GHz}$=0.64T). Table 1 shows a summary of the most recent performance of the VENUS ECR ion source. For comparison, published results from other high performance ECR ion sources are listed as reference. The ion source performance is continuing to improve as we are coupling more power into the plasma chamber. Two main magnetic confinement and heating configurations are typically used in the VENUS ECR ion source. In the single frequency heated plasma mode a minimum B field of .64 to .75 T is used, which results in a shallow magnetic field gradient at the 28 GHz resonance zone. Up to 6.5 kW of 28 GHz power has been coupled into VENUS using this mode of operation. In the double frequency mode a minimum B field of .45 T is used. This field profile results in a combination of a shallow gradient (for 18 GHz heating) and a steep gradient (for 28 GHz heating) at the resonance zone. Up to 9kW of combined 18 and 28 GHz power (a power density of about 1kW/liter) has been coupled into the VENUS plasma chamber so far. For typical 28 GHz operation in single or dual frequency mode, the sextupole magnet is energized to produce slightly above 2 Tesla at the plasma chamber wall.

Table 2: Recent Results with VENUS in comparison with other high performance sources

		VENUS	*SECRAL*[3,8]	*GTS*[11]
f(GHz)		*28 or18 +28*	*18GHz*	*18*
^{16}O	6^+	2850	2300	1950
	7^+	850	810	
^{40}Ar	12^+	860	510	380
	14^+	514	270	174
	16^+	270	73	50
	17^+	36	8.5	4.2
	18^+	1		
^{129}Xe	28^+	222		120
	29^+	168		*
	30^+	116	101	60
	31^+	86	68	40
	34^+	41	21	8
	37^+	12	5	
	38^+	7	2.4	
	42^+	.4		
^{238}U	33^+	205		
	34^+	202		
	35^+	175		
	47^+	5		
	50^+	1.9		

Beam studies with the VENUS ECR ion source

The strong confinement fields in VENUS make it possible to shift the charge state distribution over a wide range by tuning the product of plasma density and ion confinement time ($n_e\tau_i$) as well as the neutral gas density in the plasma. This tuning of plasma parameters is illustrated in figures 2, 3 and 4 for the production of argon ion beams. When both the gas flow and the magnetic confinement fields are held constant, an increase in coupled microwave power will shift the charge state distribution (CSD) to higher charge state (see Fig.2 and Fig.5a). In the case shown the charge state peak shifts from Ar^{11+} to Ar^{14+} as the power is increased from 1.6 kW to 7.6 kW. Therefore the Ar^{12+} current intensity initially increases as more power is coupled in, but eventually decreases since the increasing plasma densities enhances the ionization rate of Ar^{12+} to higher charge states (see Fig. 3).

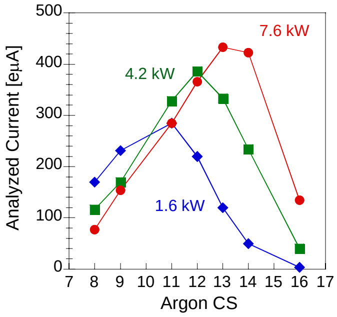

Figure 2: The argon CSD shifts from lower charge sates to higher charge state for constant gas flow and same confinement fields as the power coupled to the plasma increases.

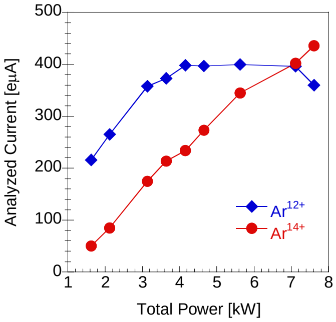

Figure 3: Dependence of Ar^{12+} and Ar^{14+} on the coupled microwave power when both, the oxygen mixing gas and the argon gas flow are held constant.

To keep the charge state distribution peaked on Ar^{12+} while increasing the microwave power, argon gas has to be added to change the charge exchange balance in the plasma.

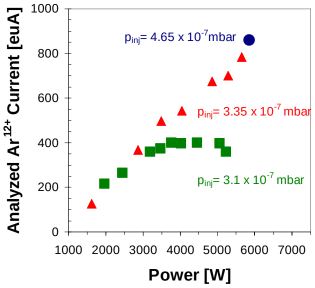

Figure 4: Dependence of the Ar^{12+} output on microwave power for 3 different argon and oxygen gas flows.

This is shown in Fig. 4 in which the dependence of the Ar^{12+} current on microwave power is graphed for different gas flow values. For reference the injection pressure measured outside the plasma chamber is stated for the different curves. For the single data point (blue circle) the gas flow for the oxygen mixing and the argon feed gas were adjusted to optimize the source for Ar^{12+} production at this power level.

By counting the bremsstrahlung emitted from the ECR ion source[12], plasma parameters can be qualitatively measured. Figure 5a shows a semi logarithmic plot of the axial bremstrahlung spectra for VENUS operated at several power levels and a similar confinement field as used for the argon data presented. The spectrum was collected for 60 seconds with a NaI detector and energy calibrated using a ^{207}Bi source[12]. As can be seen in figure 5a, the shape of the spectra is not changing with increased power, meaning that the electron energy distribution function also does not change with power. On the other hand, the total counts increase almost linearly suggesting an increase of electron density with power (Fig. 5b).

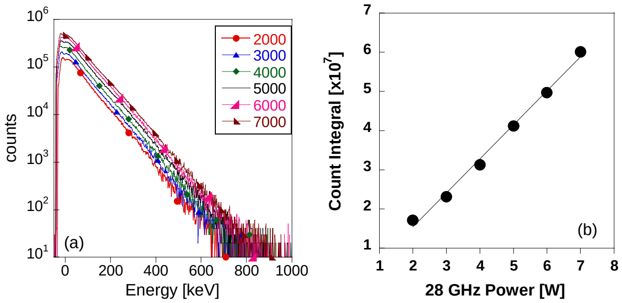

Figure 5: 5a shows the dependence of the bremsstrahlung spectra on power; in 5b the count integral is plotted in dependence of the microwave power

INTEGRATION OF THE VENUS ECR ION SOURCE INTO THE 88-INCH CYCLOTRON OPERATION

In August of 2006, the VENUS ECR ion source beam line was connected to the cyclotron injection line and in September of 2006 the first ion beam from VENUS was injected and accelerated by the 88-Inch Cyclotron. Over the last year, several cyclotron beam developments were performed using the VENUS ECR ion source. So far the Cyclotron has accelerated Ar, Kr, Xe and U beams from VENUS. Substantial gains in both intensity and energy were demonstrated for the heavy masses and very high charge state. For high charge state uranium beams such as U^{47+} 11 times more beam was extracted from the cyclotron using the VENUS ECR ion source than using the 14 GHz AECRU injector ion source. Figure 6 shows beam developments conducted with high charge state Xe beams in comparison with the beam intensities achieved using the AECRU injector ion source. 80 to 100 times more beam intensities could be extracted using the VENUS ECR ion source. In addition, the energy range for xenon has now been extended to 16.5 MeV/nucleon. For the first time neon-like xenon (Xe^{44+}) could be extracted from the cyclotron. Using Glovanisvky's diagram[13] of the $(n_e\tau_i)T_e$ criteria, this result indicates that in the VENUS source the $(n_e\tau_i)$ product has reached $2{\cdot}10^{11}$sec/cm^3.

However, at the lighter masses and lower charge states little or no gain has been achieved. Here, the intensities are limited by the acceptance of our axial line and center region not by the intensities available from the ion source. To take full advantage of the ion beam intensities available with VENUS a high voltage upgrade of the injection line and the cyclotron center region will be necessary..

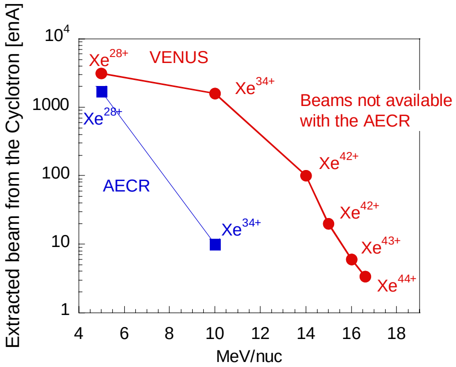

Figure 6: Extracted xenon ion beam intensities from the 88-Inch Cyclotron using the AECRU injector in comparison to the VENUS injector at various MeV/nuc and high charge state ions.

MOTIVATION AND CHALLENGES FOR 3RD AND 4TH GENERATION SC ECR ION SOURCES

Although we are still exploring the capabilities of 3rd generation sources, the anticipated current needs of future facilities will require next generation ECR ion sources As plasma density scales with the square of the frequency, at least a factor of 4 in intensity gain can be expected by going to a 4th generation ECR that can operate at twice the frequency of 3rd generation sources. The long R&D process makes it prudent to start the ground work for 4th generation sources at an early stage.

As an example the first funding for VENUS was received in 1996 to design and construct the superconducting magnet. It took another six years before the first 18 GHz plasma was ignited and another 2 years before 28 GHz was introduced, although some of this delay was funding driven. In addition, as these sources are significantly more expensive than lower frequency room temperature sources, they can only be developed and funded in the context of large heavy ion facilities. However, for these facilities the gains in performance can significantly enhance the facilities capabilities and in some cases reduce the overall accelerator construction costs, easily justifying the effort and costs of these sources.

Superconducting Magnet Technology

For 4th generation ECR ion sources the most critical technology requirement to develop is a high-field superconducting magnet system capable of confining the plasma at such high frequencies. The maximum field that can be produced in a superconducting magnet is generally limited by processes that drive the superconductor into the normal conducting state (magnet quench). To avoid quenching, the magnet design must keep the current densities and local magnetic fields at the coils below the short sample critical current in the superconductor, which depends on the type of superconductor used, the local magnetic field and the temperature. Modern ECR ion sources are all utilizing Niobium-Titanium alloy (NbTi), since it is ductile and allows simple fabrication methods for wires and cables. However, NbTi performance is ultimately limited by its upper critical field of about 10 T at 4.2 K. Therefore to extend to frequencies well above 28 GHz technology, new magnetic materials will be needed to fabricate the ECR magnet structure. The most advanced conductor for high-field applications is presently Nb_3Sn, for which the upper critical field limit increases to about 20 T at 4.2 K. Fig. 7 shows the critical current densities for both super-conducting materials in dependence of the magnetic field at the conductor at a temperature of 4.2K and 1.8K. Before these current densities can be applied to the superconducting wire used in the design of the magnet, the actual superconductor fraction of the coil packing has to be taken into account. In case of the VENUS magnet the fill factor for the sextupole wire is about 25%, which is very conservative for NbTi wire. Even for Nb_3Sn wires fill factor of 33% are routinely used. To look at the fields and current densities needed for a 56 GHz source we used a TOSCA model of VENUS to compute the fields generated when the number of ampere-turns in all coils was doubled. As the maximum surface magnetic field at any coil occurs on a sextupole coil in the VENUS geometry, these coils are the most critical component of the VENUS magnet structure and determine the maximum radial field attainable. The current NbTi sextupole magnet in VENUS reaches a maximum surface field on the coils of 6.5T, and doubling the current density increases this field to 13 T (both data points are indicated in figure 7).

The preliminary analysis shows that Nd_3Sn meets the requirement for a 56 GHz. However, the design of such a magnet would require detailed mechanical and magnetic analysis, especially since the Lorentz forces acting on the coil structure increase by a factor of 4 when the currents and the fields are doubled. In addition, Nb_3Sn is brittle and sensitive to mechanical strain making the design and fabrication of magnets more challenging. Using brittle super-conductors requires a departure from the conventional methods developed for the ductile NbTi alloy and substantial R&D will be necessary to develop such a structure. As in VENUS, the clamping of the coil structure will be crucial. The success of the VENUS magnet is based on the successful clamping of the sextupole coil using high pressure bladders[14]. LBNL has further developed this technique and applied it to Nb_3Sn magnets[15]. Using this technique, a small scale high gradient, quadrupole [15] has been fabricated and successfully tested. This technique would need to be extended for building an ECR confinement structure.

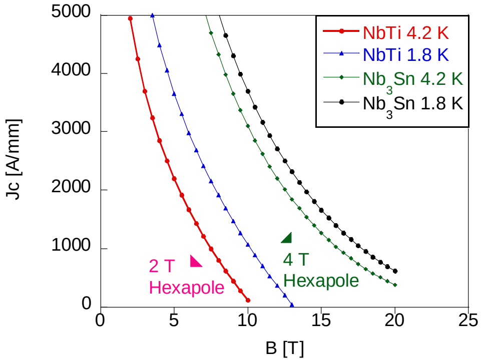

Figure 7 shows a plot of the critical current, J_c, in NbTi and Nb_3Sn for 4.2 K and 1.8 K. To the left of the curve, the material is superconducting, to the right normal conducting. Also indicated are the current densities required for the VENUS sextupole magnet to achieve 2T and 4T on the plasma chamber wall assuming a 25% filling factor.

X-ray heat load and bremstrahlung from the plasma

Bremstrahlung produced by the hot plasma electrons colliding with the plasma walls are particularly troublesome for SC ECR ion sources. Two processes in the plasma lead to the emission of bremsstrahlung. First, bremsstrahlung is created by electron-ion collisions within the plasma volume. Secondly, bremsstrahlung is emitted by electrons that are lost to the plasma chamber wall and lose their energy through interaction with the wall material. The x-rays produced by these processes can penetrate through the plasma chamber wall and are the cause of x-ray radiation in the vicinity of ECR ion sources. The x-rays can add a substantial heat load to the cryostat [12] and localized heating in the superconducting coils that may lead to quenches[16]. In addition, they can lead to the degeneration of synthetic high voltage insulator located between the warm bore of the cryostat and the plasma chamber[3]. The amount of x-rays produced when VENUS was first operated at 28 GHz was somewhat unexpected and the resulting heat load on the cryostat limited the maximum RF power that could be injected. To reduce the x-ray radiation penetrating into the cryostat, a Ta shield was developed for the VENUS ECR ion source[17]. It consists of a 2mm Ta cylinder that is placed between the plasma chamber and the cryostat. It reduces the x-ray flux roughly by a factor of 10 and allows VENUS to be tuned over a wide range of parameters. It was then found that the x-ray energy spectrum is strongly depends on the B_{min}/B_{ecr} ratio[ref]. The B_{min}/B_{ECR} ratio determines the gradient of the magnetic field at the resonance zone. Depending on this gradient the x-ray spectra can easily reach up to 1 MeV. However, x-rays with energies above 400keV are not effectively shielded by a few mm of Ta or other thin heavy metal x-ray shields and will still penetrate into the cryostat. Therefore, the heat load into the cryostat strongly depends on the B_{min}/B_{ECR} ratio used for a particular tune. For example, with the Ta liner installed an additional heat load of about 1 W/kW is added to the cryostat when a B_{min}/B_{ECR} ration of .7 is used, while for a B_{min}/B_{ECR} ratio of .45 the additional heat load is less than .1W/kW[12]. In addition, the mean electron temperature increases with frequency[12]. This temperature scaling is not yet fully understood, but will be crucial data for the design of 4th generation ECR ion sources.

Plasma chamber

Coupling enough power into 3rd and 4th generation ECR ion sources is a major challenge. The superconducting structure implies a relatively large plasma volume and this requires a large amount of 28 GHz power to achieve sufficient plasma heating In addition as the frequency is increased, more power can be coupled into the plasma without causing instabilities. Taking VENUS again as a reference, this source has been operated with up to about 9 kW of RF power so far (about 1 kW/liter) and is clearly not at the saturation point of the ion source. This is not surprising considering that the 14 GHz AECRU is operated with up to 2.5 kW/liter before reaching saturation.

One challenge for the high power source operation is avoid local burn out of the plasma chamber due to the inhomogeneous heating distribution onto the plasma chamber walls due to particles losses. The weakest regions of the magnetic confinement field are three local magnetic field minima, where the large gradient in the solenoid field produces a radial component that partially cancels the radial field produced by the sextupole. On these spots the plasma confinement is compromised and localized heating of the plasma chamber walls occurs which can lead to burn out of the plasma chamber. Therefore the engineering design of the plasma chamber cooling needs to be carefully optimized to withstand this localized heat load. For this purpose, the VENUS plasma chamber is made out of aluminum and has been optimized to maximize the water flow around the plasma chamber. A similar or better design will be needed for the 4th generation ECR ion sources.

Beam Transport

Superconducting ECR ion sources produce several mA of heavy ions, and the extracted ion beams are highly space-charge dominated. In addition, they are extracted from a high magnetic field region. As the extracted beam is accelerated through this decreasing magnetic field, an axial rotation is introduced due to canonical angular momentum conservation, which results in transverse emittance growth. Therefore, as the extraction field is increased to operate the source at higher frequency an emittance growth is observed. As an example Figure 8 shows a series of emittance measurements over several days for medium charge state Xe ions extracted when VENUS was operated at 18 GHz fields and 28 GHz fields.

As observed in other sources the data in figure 8 shows significant spread reflecting the plasma stability of different tunes[18]. Nevertheless, a clear trend to higher emittances when higher magnetic fields are used can be seen. This trend is likely to be continued for even higher field sources and will require reliable simulation[19,20] of ion beam extraction and transport in low energy beam transport line design to minimize further emittance growth.

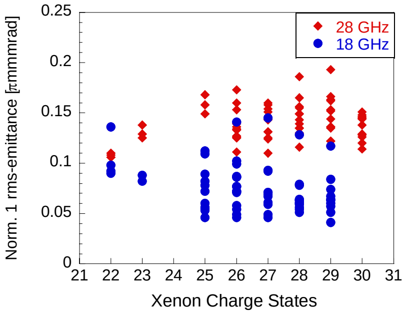

Figure 8: Measured emittance of medium charge state xenon ion beams extracted from VENUS for 18 and 28 GHz operation.

ACKNOWLEDGMENTS

This work was supported by the Director, Office of Energy Research, Office of High Energy and Nuclear Physics, Nuclear Physics Division of the U.S. Department of Energy under Contract DE AC03-76SF00098

REFERENCES

[1] R. Geller, F. Bourg, P. Briand, J. Debernardi, M. Delaunay, B. Jacquot, P. Ludwig, R. Pauthenet, M. Pontonnier, and P. Sortais, Proceedings of the Proceedings of the 11th International Conference on ECR Ion Sources Their Applications, East Lansing, MI, MSUCP-47, 1987 1-33

[2] P. A. Zavodszky, B. Arend, D. Cole, J. DeKamp, G. Machicoane, F. Marti, P. Miller, J. Moskalik, J. Ottarson, J. Vincent, and A. Zeller, Rev. Sci. Instrum. **77**, 03A334 (2006).

[3] H. W. Zhao, L. T. Sun, X. H. Guo, X. Z. Zhang, Z. M. Zhang, P. Yuan, D. Z. Xie, J. Y. Li, Y. C. Feng, W. He, M. T. Song, X. X. Li, Y. Cao, H. Wang, B. H. Ma, W. Lu, W. L. Zhan, and B. W. Wei, Journal of HEP&NP, Chinese Physical Society **31**, 8-12 (2006).

[4] C. Lyneis, D. Leitner, D.S. Todd, G. Sabbi, S. Prestemon, S Caspi, and P. Ferracin, RSI, submitted (2008).

[5] S. Gammino, Journal of HEP&NP, Chinese Physical Society **31**, 137 (2007).

[6] P. A. Zavodszky, B. Arend, D. Cole, J. DeKamp, G. Machicoane, F. Marti, P. Miller, J. Moskalik, J. Ottarson, J. Vincent, and A. Zeller, Proceedings of the 18th International Conference on Cyclotrons and Their Applications (CYCLOTRONS 2007), Giardini Naxos, Messina, Italy, 2008

[7] S. Gammino, G. Ciavola, L. Celona, L. Torrisi, S. Passarello, L. Andó, M. Cavenago, A. Galatà, P. Spaedtke, K. Tinschert, R. Lang, R. Iannucci, R. Leroy, C. Barue, D. Hitz, P. Seyfert, H. Koivisto, P. Suominen, O. Tarvainen, H. Beijers, S. Brandenburg, D. Vanrooyen, C. Hill, D. Kuchler, H. Homeyer, J. Röhrich, L. Schachter, and S. Dobrescu, Proceedings of the 18th International Conference on Cyclotrons and Their Applications (CYCLOTRONS 2007), Giardini Naxos, Messina, Italy, 2008

[8] H. W. Zhao, L. T. Sun, X. H. Guo, X. Z. Zhang, Z. M. Zhang, P. Yuan, D. Z. Xie, J. Y. Li, Y. C. Feng, W. He, M. T. Song, X. X. Li, Y. Cao, H. Wang, B. H. Ma, W. Lu, W. L. Zhan, and B. W. Wei, Proceedings of the 18th International Conference on Cyclotrons and Their Applications (CYCLOTRONS 2007), Giardini Naxos, Messina, Italy, 2008

[9] T. Nakagawa, Y. Higurashi, M. Kidera, T. Aihara, M. Kase, A. Goto, and Y. Yano, Rev. Sci. Instrum. **77**, 03A304 (2006).

[10] D. Leitner, D.S. Todd, M.L. Galloway, and C.M. Lyneis, Journal of HEP&NP, Chinese Physical Society **31**, 1-7 (2006).

[11] D. Hitz, A. Girard, K. Serebrennikov, G. Melin, D. Cormier, J. M. Mathonnet, L. Sun, J. P. Briand, and M. Benhachoum, RSI **75** (5), 1403 (2004).

[12] D. Leitner, C.M. Lyneis, H. Koivisto, T. Ropponen, J. Ropponen, D.S. Todd, J.Y. Benitez, and S. Gammino, RSI (in print) (2008).

[13] K.S. Golovanivsky, Instrumentations and Experimental Techniques **28** (5), 989 (1986).

[14] C. E. Taylor, S. Caspi, M. Leitner, S. Lundgren, C. Lyneis, D. Wutte, S.T. Wang, and J.Y. Chen, IEEE Transactions on Applied Superconductivity **10** (1), 224 (2000).

[15] P. Ferracin, G. Ambrosio, E. Barzi, S. Caspi, D. R. Dietderich, S. Feher, S. A. Gourlay, A. R. Hafalia, C. R. Hannaford, J. Lizarazo, A. F. Lietzke, A. D. McInturff, G. L. Sabbi, and A. V. Zlobin, IEEE Transactions On Applied Superconductivity **17** (2) (2007).

[16] S. Gammino, G. Ciavola, L. Celona, P. Romano, L.Torrisi, D. Hitz, A. Girard, and G. Melin, Proceedings of the Cyclotrons and their Applications 2001, East Lansing, Michigan, AIP, 600, 2001 223-227

[17] C. M. Lyneis, D. Leitner, O. Tarvainen, D. Todd, S. Virostek, T. Loew, and A. Heinen, RSI **77** (03A342) (2006).

[18] D. Wutte, M. Leitner, and C.M. Lyneis, Physica Scripta **T92**, 247 (2001).

[19] P. Spaedtke, RSI, submitted (2008).

[20] D.S. Todd, D. Leitner, C. Lyneis, and D.P. Grote, RSI, submitted (2008).